Voltage Profile Optimization of Active Distribution Networks Considering Dispatchable Capacity of 5G Base Station Backup Batteries

Yiyao Zhou, Qianggang Wang, Yao Zou, Yuan Chi, Niancheng Zhou, Xuefei Zhang, Chen Li, and Qinqin Xia

***Abstract*—The penetration of distributed energy resources (DERs) and energy-intensive resources is gradually increasing in active distribution networks (ADNs), which leads to frequent and severe voltage violation problems. As a densely distributed flexible resource in the future distribution network, 5G base station (BS) backup battery is used to regulate the voltage profile of ADN in this paper. First, the dispatchable potential of 5G BS backup batteries is analyzed. Considering the spatial-temporal characteristics of electric load for 5G BS, the dispatchable capacity of backup batteries at different time intervals is evaluated based on historical heat map data. Then, a voltage profile optimization model for ADN is established, consisting of 5G BS backup batteries and other voltage regulation resources. In this model, the charging/discharging behavior of backup batteries is based on its evaluation result of dispatchable capacity. Finally, the range of charging/discharging cost coefficients of 5G BS that benefits ADN and 5G operators are analyzed respectively. Further, an incentive policy for 5G operators is proposed. Under this policy, the charging/discharging cost coefficients of 5G BS can achieve a win-win situation for ADN and 5G operators. As an emerging flexible resource in ADN, the effectiveness and economy of 5G BS backup batteries participating in voltage profile optimization are verified in a test distribution network.**

***Index Terms*—Voltage profile optimization, 5G base station (BS) backup battery, active distribution network (ADN), flexible resource, voltage violation.**

NOMENCLATURE

$\pi(j), \delta(j)$	Sets of parent and child nodes of j
$\Delta\tau$	Duration of charging/discharging
$\eta_{BS,j,a}^{ch}$, $\eta_{BS,j,a}^{dis}$	Charging and discharging efficiencies of the a^{th} 5G base station (BS) for node j
$\eta_{ESS,j}^{ch}$, $\eta_{ESS,j}^{dis}$	Charging and discharging efficiencies of energy storage system (ESS) for node j
$a_{s,j,t}^{OLTC}$, $a_{s,j,t}^{CB}$	Tap status of on-load tap changer (OLTC) and capacitor bank (CB) for node j at t
$b_{OLTC,j,t}^{IN}$, $b_{OLTC,j,t}^{DE}$	Increasing and decreasing statuses of OLTC for node j at t
$b_{CB,j,t}^{IN}$, $b_{CB,j,t}^{DE}$	Increasing and decreasing statuses of CB for node j at t
$b_{ESS,j,t}^{ch}$, $b_{ESS,j,t}^{dis}$	Charging and discharging states of ESS for node j at t
$b_{BS,j,a,t}^{ch}$, $b_{BS,j,a,t}^{dis}$	Charging and discharging states of the a^{th} 5G BS for node j at t
C_{loss}, C_{ESS}, C_Q^{SVC}, C_{CB}, C_{OLTC}	Cost coefficients of loss, ESS, static var compensator (SVC), CB, and OLTC
$C_{ch,t}^{BS}$, $C_{dis,t}^{BS}$,	Charging and discharging cost coefficients of 5G BS
$C_{BS,j,a}^{deg}$	Degradation cost coefficient of the a^{th} 5G BS for node j
$C_{BS,j,t}^{deg,\max}$	The maximum degradation cost coefficient of 5G BS for node j
$DoD_{BS,j,a}^{(\cdot)}$	Depth of charging/discharging (DoD) of the a^{th} 5G BS for node j
$DoD_{BS,j,t}^{(\cdot),up}$	Upper limit of DoD of 5G BS for node j at t
$E_{j,t}^{ESS}$	Electric power of ESS for node j at t
$E_j^{ESS,\max}$, $E_j^{ESS,\min}$	Upper and lower limits of $E_{j,t}^{ESS}$
$E_{j,to}^{BS}$	Initial electric power of 5G BS backup batteries for node j at t
$E_{j,t}^{BS,n}$	The minimum demand power of 5G BS for node j at t
$E_{j,t}^{BS}$	Aggregated electric power of 5G BS backup batteries for node j at t
$E_{j,t}^{BS,d}$	Aggregated dispatchable capacity of 5G BS backup batteries for node j at t
$E_{a,0}^{BS}$	Rated backup battery capacity of the a^{th} 5G BS
$E_{BS,j,a}^{ch}$, $E_{BS,j,a}^{dis}$	Charging and discharging electric power of the a^{th} 5G BS for node j

Manuscript received: July 28, 2022; revised: October 27, 2022; accepted: February 22, 2023. Date of CrossCheck: February 22, 2023. Date of online publication: May 1, 2023.

This work was supported by the National Natural Science Foundation of China (No. 52077017).

Y. Zhou, Q. Wang, Y. Zou, Y. Chi (corresponding author), N. Zhou, X. Zhang, C. Li, and Q. Xia are with the School of Electrical Engineering, Chongqing University, Chongqing, China (e-mail: yiyaozhou@cqu. edu. cn; qianggang1987@cqu. edu. cn; zoyire@foxmail. com; chiyuanee@cqu. edu. cn; cee_nczhou@cqu. edu. cn; zhangxuefei@cqu. edu. cn; menghuanluren1216@163. com; xiaquine@cqu.edu.cn).

DOI: 10.35833/MPCE.2022.000453

F_{loss}, F_{ESS}, F_{SVC}, F_{OLTC}, F_{CB} Costs of network loss, ESS, SVCs, OLTC and CBs

$F_{re,BS}$ Replacement cost of 5G BS backup batteries

$F_{j,deg}$ Degradation cost of backup batteries for 5G BS

$F_{j,ope}$ Revenue of 5G operator

k_s Difference of OLTC change ratio square between s and $s-1$ taps

$k_{\min}$ OLTC change ratio square corresponding to the minimum tap

$l_{ij,t}$ Square of current for branch ij at t

$l_{ij,\max}$, $l_{ij,\min}$ Upper and lower limits of $l_{ij,t}$

$n_{j,t}^{OLTC}$, $n_{j,t}^{CB}$ Taps of OLTC and CB for node j at t

$N_{OLTC}^{\max}$, $N_{CB}^{\max}$ Tap limits of OLTC and CB

$\Delta n_{j,T}^{OLTC,\max}$, $\Delta n_{j,T}^{CB,\max}$ Operation limits of OLTC and CB for node j at the T^{th} time interval

$N_{j,t}^{BS,d}$ Number of 5G BSs with dispatchable capacity for node j at t

$P_{j,t}^{PV}$, $P_{j,t}^{ESS}$, $P_{j,t}^{BS}$ Injected active power of PV, ESS, and 5G BS backup batteries for node j at t

P_a^{BS} Electric load of the a^{th} 5G BS

$P_{ESS,j,t}^{ch}$, $P_{ESS,j,t}^{dis}$ Charging and discharging power of ESS for node j at t

$P_{ESS,j}^{ch,\max}$, $P_{ESS,j}^{dis,\max}$ The maximum values of $P_{ESS,j,t}^{ch}$ and $P_{ESS,j,t}^{dis}$

$P_{j,a,t}^{BS}$ Electric load of the a^{th} 5G BS for node j at t

$P_{BS,j,a}^{conver}$ Output power of the a^{th} 5G BS converter for node j

$P_{BS,j,a,t}^{ch}$, $P_{BS,j,a,t}^{dis}$ Charging and discharging power of the a^{th} 5G BS for node j at t

$P_{BS,j,a,t}^{ch,\max}$, $P_{BS,j,a,t}^{dis,\max}$ The maximum values of $P_{BS,j,a,t}^{ch}$ and $P_{BS,j,a,t}^{dis}$

$P_{j,t}$, $Q_{j,t}$ Net injected active and reactive power of node j at t

$P_{ij,t}$, $Q_{ij,t}$ Active and reactive power of branch ij at t

$P_{j,t}^{L}$, $Q_{j,t}^{L}$ Active and reactive loads of node j at t

$Q_{j,t}^{PV}$, $Q_{j,t}^{CB}$, $Q_{j,t}^{SVC}$ Injected reactive power of PV, CB, and SVCs for node j at t

$Q_j^{SVC,\max}$, $Q_j^{SVC,\min}$ Upper and lower limits of $Q_{j,t}^{SVC}$

q_{step}^{CB} Step reactive power of CB

r_{ij}, x_{ij} Resistance and reactance of branch ij

S^N, j Set and index of nodes in ADN

S^B, ij Set and index of branches in ADN

S^{ESS}, S^{BS}, S^{PV}, S^{SVC}, S^{CB}, S^{OLTC} Sets of ESS, 5G BS, PV, SVC, CB, and OLTC in ADN

$SOC_{a,L,t}^{BS,n}$ State of charge (SOC) value of the minimum capacity required of the a^{th} 5G BS at t

$SOC_{j,a,L,t}^{BS,n}$ SOC value of the minimum capacity required of the a^{th} 5G BS for node j at t

T, t Set and index of time interval

$T_{a,d}$ The maximum power interruption time of the a^{th} 5G BS

$T_{a,re}^{BS}$, $T_{a,re}^{BS,ESS}$ The maximum power interruption time considering the power supply reliability demand and the reliability rate of backup batteries for the a^{th} 5G BS

$v_{j,t}$ Square of voltage for node j at t

$v_{j,\max}$, $v_{j,\min}$ Upper and lower limits of $v_{j,t}$

$v_{pri,t}$ Square of voltage on primary side at t

I. Introduction

THE development of distributed energy resources (DERs) has accelerated the transformation of distribution networks from passive to active [1]. Active distribution networks (ADNs) have high flexibility and reliability, but the uncertainty and fluctuation of DERs also threaten the safe and economic operation of ADN. In particular, the voltage violation and fluctuation are more severe for low-voltage (LV) distribution networks with high-penetration photovoltaics (PVs) and electric vehicles (EVs) [2].

In the classic volt-var control (VVC) architecture, ADN improves the voltage quality by actively controlling conventional voltage regulation devices such as on-load tap changer (OLTC), capacitor bank (CB), energy storage system (ESS), and static var compensator (SVC) [3]. However, the above devices cannot respond frequently due to the limitation of operation time and service life, which makes it difficult for them to alleviate the influence of distributed generation (DG) output and load rapid change on voltage. DG, represented by PVs, can rapidly and continuously adjust voltage through active power curtailment (APC) or reactive power compensation (RPC) [4]. ADN often coordinates PVs with conventional devices through a multi-level control architecture, where the local voltage control of PV improves the response speed of ADN [5], and the conventional devices make up for the insufficient inverter capacity and limited night voltage support. The wide application of soft open point (SOP) also provides a new solution to the ADN voltage problem. The power flow transfer capability of SOP can be used for network reconfiguration to balance the branch power variation caused by DG output and load fluctuation [6]. In addition, in order to accurately control the voltage of high-penetration ADN, the existing research also divides the control time scale according to the response characteristics of different voltage regulation devices. In general, the time scale of discrete regulation device is larger, and the time scale of continuous regulation device is smaller. The development of data-driven technology has further extended the time scale of ADN voltage control to the real-time stage [7]. Reference [8] provides a basis for PV online response by training historical voltage data offline through deep reinforcement learning. However, it is difficult for the conventional VVC to solve the ADN voltage problem completely, and more flexible resources are required to participate in the

management of ADN [9].

Flexible resources such as EVs and air conditioners have played an active role in the optimization of voltage profiles and operation costs in ADN [10]-[13]. As a significant voltage regulation resource in ADN, EVs can not only adjust the charging/discharging behavior in response to electricity price incentives [14], [15], but also have a certain reactive power support capability. One of its limitations is that its voltage regulation decision is affected by the multi-dimensional uncertainty factors of the traffic-road-grid. Similar to EVs, the air conditioner is also a flexible resource on the demand side. Under the premise of maintaining a comfortable room temperature, the compressor speed can be adjusted through demand response, thereby changing the operation power of the air conditioner [16], and participating in voltage profile optimization of ADN. With the development of demand response technology, more and more flexible resources will participate in the active management of distribution networks. Especially, 5G base station (BS) shows great potential in providing auxiliary services for ADN [17], which can provide large-capacity power support steadily even at night.

5G communication provides high bandwidth, high capacity, and low latency communication, which makes it a trend in communication networks [18], [19]. Since a 5G BS has a narrower frequency band, more 5G BSs (3-4 times of the 4G counterpart) are needed to achieve the same coverage effect [20]. Therefore, its installations will inevitably increase explosively with the promotion and development of 5G technology. By the end of 2021, a total of 1.425 million 5G BSs have been built and opened in China [21]. It is estimated that the number of 5G BSs built in China will exceed 10 million by 2030 [22]. The power consumption cost of 5G BS is as high as 15% of the network maintenance cost of operators [23], [24]. Huge electricity bills not only increase the cost of operators, but also hinder the promotion and development of 5G technology.

At present, there are mainly three ways for 5G operators to reduce the maintenance costs: ① planning the location of 5G BS according to users' needs, and reducing the number of 5G BS layouts under the premise of ensuring communication coverage [25]; ② integrating distributed renewable energy sources in 5G BS to reduce the cost of purchasing electricity from the main network [26]; ③ optimizing the power consumption of 5G BS through active energy efficiency management technologies such as BS dormancy [27] and power amplifier voltage regulation [28]. In addition, providing auxiliary services for ADN can generate additional revenue to cover the operation costs for BS operators. 5G BS is equipped with sufficient backup batteries to ensure 99.999% power supply reliability [29]. Active energy efficiency management technologies reduce the capacity requirement of backup batteries for 5G BS, making it a promising flexible resource in ADN. Previous research has shown that the dispatchable capacity of 5G BS backup batteries can be redistributed according to the dynamic pricing of smart grid, and two-way energy transactions between 5G BS and smart grid can be realized [30]. Reference [31] proposes the concept of spatial-temporal energy management for BSs, which manages the power consumption of devices in 5G BS according to the real-time electricity price. 5G BSs can determine whether to respond to the incentive policy of ADN in combination with its own electric load and the backup battery capacity demands. Nonetheless, BS operators will never prioritize auxiliary services over the communication quality. Therefore, it is crucial to analyze the electric load and dispatchable capacity of 5G BS backup batteries. In our previous study [32], we established an electric load demand model of 5G BS based on data flow analysis. Reference [33] considers the effect of power supply interruption and backup batteries on the reliability of 5G BS power consumption, and evaluates the dispatchable capacity of 5G BS under different reliability levels. 5G BS backup batteries are essentially a kind of dynamic energy storage resource. The above studies lay a theoretical foundation for 5G BS to participate in the active management of ADN. The backup batteries have been proven to effectively adjust the frequency of the power system [34], but, to the best of our knowledge, there is no research on 5G BS as a voltage optimization service provider.

To address the voltage violation problem caused by the fluctuation and uncertainty of DER output in ADN, this paper considers 5G BS backup battery as a new flexible resource and uses it to optimize the voltage profile of ADN. The main contributions of this paper are as follows.

1) A novel evaluation method is proposed for the dispatchable capacity of 5G BS backup batteries at different time intervals. The method is based on the analyzed electric load composition of 5G BS and the uncertainty of 5G users' behavior, as well as the forecasted electric load of 5G BS using historical heat map data.

2) The dispatchable capacity of 5G BS backup batteries is used for voltage profile optimization of ADN, which expands the type of voltage regulation resources in ADN and explores a new application for backup batteries.

3) An incentive policy that can achieve a win-win situation for both parties is proposed, based on a detailed analysis on the range of charging/discharging cost coefficients for 5G BS that benefit ADN and 5G operators. This win-win incentive mechanism enhances the rationality for 5G BS to participate in ADN voltage regulation.

The rest of this paper is organized as follows. Section II analyzes the dispatchable potential of 5G BS backup batteries. Section III establishes a voltage profile optimization model for ADN with 5G BS backup batteries. Then, an incentive policy for 5G BS to participate in the voltage profile optimization of ADN is proposed in Section IV. In Section V, the results of our numerical study are shown and analyzed. Section VI concludes this paper with the final remarks.

II. Dispatchable Potential Analysis of 5G BS Backup Batteries

A. Electric Load Composition

The electric loads of 5G BS can be divided into DC load and AC load according to the power supply mode. The AC load is the electric device that maintains the indoor environment of 5G BS, such as air conditioners and illumination devices. The DC load is mainly the communication devices re-

sponsible for sending/receiving wireless signals and processing [35], such as active antenna unit (AAU), base band unit (BBU), synchronous digital hierarchy (SDH) system, wavelength division multiplexing (WDM) system, optical distribution frame (ODF), and digital distribution frame (DDF). The distribution network is the main power supply for 5G BS. In the event of distribution system failure, the batteries provide a backup power supply path for the 5G BS [33] to ensure high-quality communication services. The basic components of a 5G BS are shown in Fig. 1, where FE and GE are short for fast Ethernet and Gigabit Ethernet, respectively.

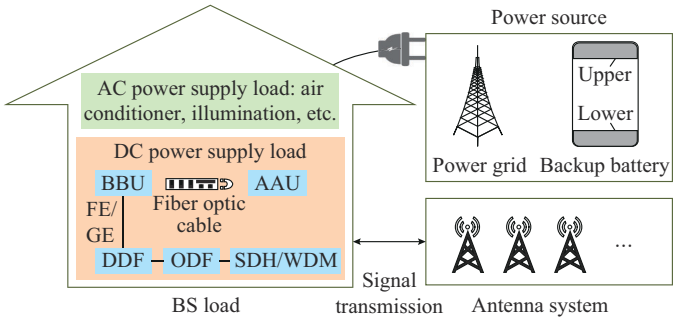

Fig. 1. Basic components of 5G BS.

Most of the devices in 5G BS operate uninterruptedly. Among the DC loads, the AAU, which is positively correlated with the communication load, accounts for 75% [36] of communication consumption, while the BBU, which is also affected by the communication load, accounts for a slight portion (5%) [36]. AC load is relatively stable (power consumption is about 2 kW), which is the baseline load of the 5G BS and is not affected by the communication load. In general, the total electric load of 5G BS is linearly related to the communication load, as shown in Fig. 2, where $P_{BS}(t)$ is the electric load of 5G BS at t; $C_{BS}(t)$ is the communication load connected to 5G BS at t; $C_{\max}$, C_{base} and $P_{\max}$, P_{base} are the maximum/baseline communication load and power consumption of 5G BS, respectively.

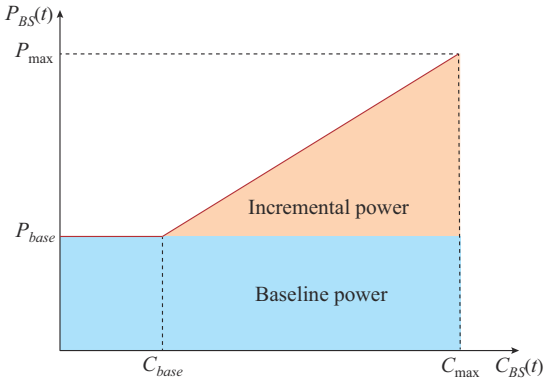

Fig. 2. Power consumption in 5G BS.

The total electric load of 5G BS consists of baseline load and incremental load, which can be expressed as:

$$P_{BS}(t)=P_{base}+\lambda_{BS}C_{BS}(t) \tag{1}$$

where λ_{BS} is slope of the $P_{BS}(t)$-$C_{BS}(t)$ curve.

B. Electric Load Characteristics of 5G BS

Since the communication load varies with the number and service demands of users in the coverage area of a 5G BS, the electric load of 5G BS shows significant spatial-temporal characteristics.

The number of users connected to the 5G BS changes regularly. During the morning peak (hours 8-10), a large number of users move from residential areas to office areas due to work needs, while there is a reverse flow during the evening peak (hours 18-20). This tidal effect causes the communication load of the 5G BS to shift regionally at a specific time interval, and makes the electric load of 5G BS change consistently. Figure 3 shows the daily curves of the electric load and communication load of 5G BS in a typical area.

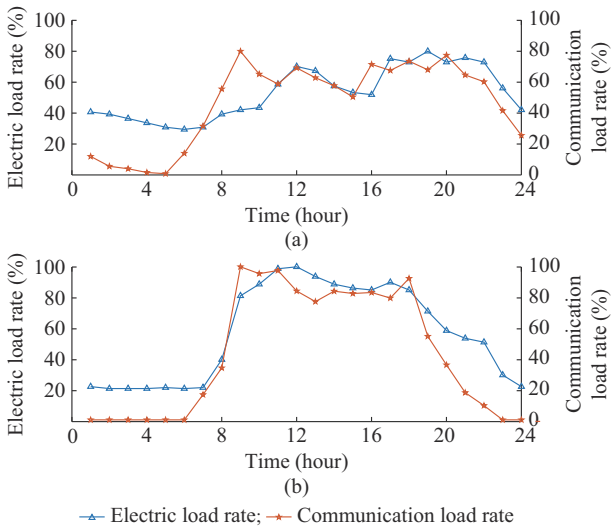

Fig. 3. Daily curves of electric load and communication load of 5G BS in a typical area. (a) Residential area. (b) Office area.

There are spatial-temporal structural changes in the service demands of users connected to the 5G BS.

The demand of users for 5G service is affected by their behaviors of using communication terminals. In office areas, terminals are generally activated during leisure time, not working hours. In residential areas, terminals are generally activated during holidays and leisure time, not working days and sleep time. Among all 5G application demands of users, video service has the highest bandwidth demands and has the largest impact on communication load. In the future, video services will account for more than 90% of 5G applications [32]. Changes in the structure of service demands for users will affect the bandwidth occupancy ratio and sub-bandwidth occupancy number of 5G BS, which will make the spatial-temporal characteristics of communication load and electric load for 5G BS more significant.

C. Dispatchable Capacity Analysis

Due to the spatial-temporal characteristics of electric load, the required capacity of 5G BS backup battery varies at each time interval. The minimum backup battery capacity depends on the maximum power supply interruption time and power load curve of the 5G BS, which can be calculated by [33]:

$$SOC_{a,L,t}^{BS,n}=\frac{\int_{t}^{t+T_{a,d}}P_{a}^{BS}(\tau)\,\mathrm{d}\tau}{E_{a,0}^{BS}}\times 100\% \tag{2}$$

The value of $T_{a,d}$ is determined by the reliability index and the battery reliability rate of 5G BS. The premise of backup batteries participating in ADN voltage optimization is to ensure the power supply reliability of 5G BS. During the failure of the distribution system, the power supply time of backup batteries of the a^{th} BS should not be less than $T_{a,d}$.

$$T_{a,d}=\max\{T_{a,re}^{BS},T_{a,re}^{BS,ESS}\} \tag{3}$$

The value of P_a^{BS} is determined by the communication load of 5G BS. The tidal effect of 5G users makes the communication load of 5G BSs in office areas and residential areas have obvious changes at a specific time interval. However, the communication loads of 5G BSs located in certain areas (shopping malls, hospitals, etc.) are uncertain because of the irregular flow of 5G users. Baidu heat map is a tool that can utilize the geographic information generated by mobile users when using location-based service applications (including active and background applications) to represent different degrees of crowd aggregation at a certain time interval in an area [32]. Therefore, it is adopted to reflect the communication load of 5G BS. Figure 4 shows an example of a heat map in residential area, where different colors correspond to the crowd aggregation degree at different time intervals. The darker the color, the denser the crowd. By extracting the color information in each pixel of the map and superimposing the same color pixels, the total amount of crowd aggregation in the area at different time intervals can be obtained. The electric load of 5G BS is further calculated according to the method of data flow analysis [32] in the previous study.

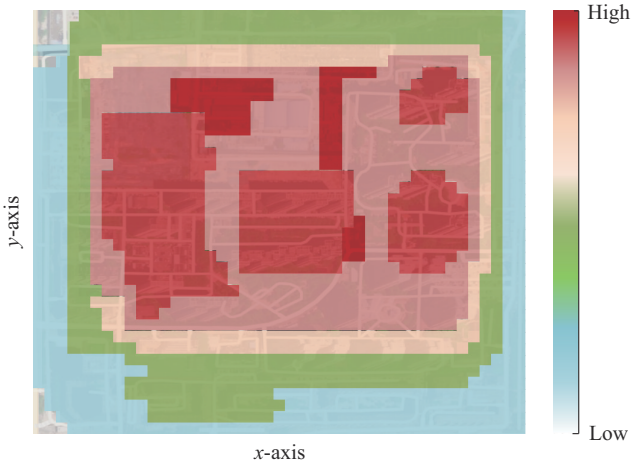

Fig. 4. Example of heat map with color corresponding to crowd aggregation degree.

When the 5G BS is working normally, the area covered by the transmitted signal is a regular hexagon, and the coverage area of a single 5G BS is about 0.104 km^2 [37]. Therefore, multiple 5G BSs need to be planned for the same node in ADN to ensure the quality of communication services.

When 5G BS backup batteries participate in the voltage profile optimization of ADN, the dispatchable capacity of 5G BS backup batteries connected to the same node can be aggregated as:

$$E_{j,t}^{BS,d}=\sum_{a=1}^{N_{j,t}^{BS,d}}(1-SOC_{j,a,L,t}^{BS,n})E_{a,0}^{BS} \tag{4}$$

D. Dispatchable Capacity Evaluation of 5G BS Backup Batteries

Figure 5 shows the evaluation system of dispatchable capacity for 5G BS backup batteries. First, collect historical heat map data of different types of areas (residential, commercial, and office areas), and calculate historical crowd aggregation data. Different neural network models are trained for different regions, working day, and non-working day to predict crowd aggregation data. Furthermore, the electric load of 5G BS is calculated according to the forecasted results, and the maximum power interruption time is set up according to the reliability index and battery reliability rate of all 5G BSs. Finally, the capacity demand of each 5G BS backup battery is calculated according to (2) - (4), the BSs with the dispatchable capacity of 5G BS backup batteries are selected and the aggregated dispatchable capacity of 5G BS backup batteries at each node of ADN is calculated according to (4).

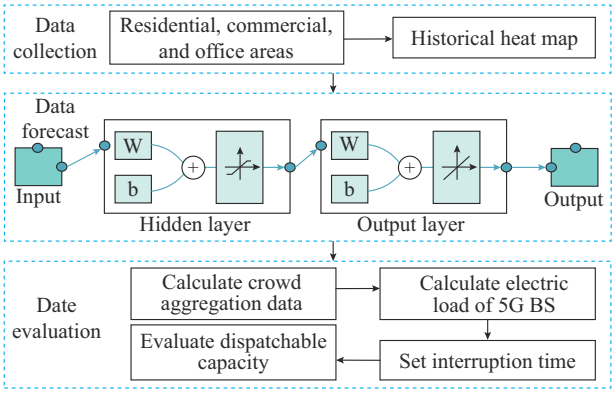

Fig. 5. Evaluation system of dispatchable capacity for 5G BS backup batteries.

III. Voltage Profile Optimization Model for ADN Considering 5G BS Backup Batteries

The compact form of the voltage profile optimization model for ADN can be expressed as:

$$\begin{cases}\min \boldsymbol{F}(\boldsymbol{x}_t)\\ \text{s.t. } \boldsymbol{h}(\boldsymbol{x}_t)=\boldsymbol{0}\\ \quad \boldsymbol{g}(\boldsymbol{x}_t)\le \boldsymbol{a}\\ \quad \|\boldsymbol{A}_{ij,t}\boldsymbol{x}_t\|\le \boldsymbol{b}_{ij,t}^{\mathrm{T}}\boldsymbol{x}_t \quad \forall ij\in S^B\end{cases} \tag{5}$$

where $\boldsymbol{F}(\boldsymbol{x}_t)$ is the objective function, including the costs of network loss and voltage regulation resources; $\boldsymbol{x}_t$ denotes the decision variables; and the inequality and equality vector constraints are affected by power flow and voltage regulation resources, and the specific constraints of each element will be described in the following subsections.

The objective function and constraints describe the voltage profile optimization problem of ADN as a mixed integer second-order cone programming (MISOCP) problem, which can be solved by commercial software.

A. Objective Function

The objective function is the cost of network loss and flexible resources, which can be expressed in (6)-(11).

$$F = F_{loss} + F_{ESS} + F_{BS} + F_{SVC} + F_{CB} + F_{OLTC} \tag{6}$$

$$F_{loss} = C_{loss} \sum_{T=1}^{24} \sum_{t \in T} \sum_{j \in S^B} l_{ij,t} r_{ij} \tag{7}$$

$$F_{ESS} = C_{ESS} \sum_{T=1}^{24} \sum_{t \in T} \sum_{j \in S^{ESS}} (b_{ESS,j,t}^{ch} P_{ESS,j,t}^{ch} + b_{ESS,j,t}^{dis} P_{ESS,j,t}^{dis}) \tag{8}$$

$$F_{BS} = \sum_{T=1}^{24} \sum_{t \in T} \sum_{j \in S^{BS}} C_{ch,t}^{BS} P_{BS,j,t}^{ch} + \sum_{T=1}^{24} \sum_{t \in T} \sum_{j \in S^{BS}} C_{dis,t}^{BS} P_{BS,j,t}^{dis} \tag{9}$$

$$F_{SVC} = C_Q^{SVC} \sum_{T=1}^{24} \sum_{t \in T} \sum_{j \in S^{SVC}} Q_{j,t}^{SVC} \tag{10}$$

$$F_{CB} = C_{CB} \sum_{T=1}^{24} \sum_{t \in T} \sum_{j \in S^{CB}} (b_{CB,j,t}^{IN} + b_{CB,j,t}^{DE}) \tag{11}$$

$$F_{OLTC} = C_{OLTC} \sum_{T=1}^{24} \sum_{t \in T} \sum_{j \in S^{OLTC}} (b_{OLTC,j,t}^{IN} + b_{OLTC,j,t}^{DE}) \tag{12}$$

It is noteworthy that $C_{ch,t}^{BS}$ and $C_{dis,t}^{BS}$ are time-varying values, and the method for determining their values is described in detail in Section IV.

B. Constraints

The constraints of the voltage optimization model for ADN include power flow constraints, capacity and operation constraints of voltage regulation resources (ESSs, 5G BS backup batteries, PVs, SVCs, CBs, and OLTCs).

1) Power Flow Constraints

$$\begin{cases} \sum_{i \in \pi(j)} (P_{ij,t} - l_{ij,t} r_{ij}) + P_{j,t} = \sum_{k \in \delta(j)} P_{jk,t} \\ \sum_{i \in \pi(j)} (Q_{ij,t} - l_{ij,t} r_{ij}) + Q_{j,t} = \sum_{k \in \delta(j)} Q_{jk,t} \\ P_{j,t} = P_{j,t}^{PV} + P_{j,t}^{ESS} + P_{j,t}^{BS} - P_{j,t}^{L} \\ Q_{j,t} = Q_{j,t}^{PV} + Q_{j,t}^{CB} + Q_{j,t}^{SVC} - Q_{j,t}^{L} \\ v_{j,t} = v_{i,t} - 2(P_{ij,t} r_{ij} + Q_{ij,t} x_{ij}) + l_{ij,t}(r_{ij}^2 + x_{ij}^2) \end{cases} \quad \forall ij \in S^B, \forall j \in S^N \tag{13}$$

$$l_{ij,t} = \frac{P_{ij,t}^2 + Q_{ij,t}^2}{v_{i,t}} \tag{14}$$

$$\begin{cases} l_{ij,\min} \le l_{ij} \le l_{ij,\max} \\ v_{j,\min} \le v_j \le v_{j,\max} \end{cases} \tag{15}$$

Formulas (13)-(15) are Distflow branch constraints, which are employed to illustrate the radial topology feature for ADN [38]. Formula (13) is for active power balance, reactive power balance, and voltage balance. Formula (15) is the security constraint of ADN. The nonconvexity results from (14), and the second-order cone relaxation technique efficiently relaxes the original model into (16). The exactness of this relaxation and its duality with the original model have been rigorously proved in [39].

$$\left\| \begin{matrix} 2P_{ij,t} \\ 2Q_{ij,t} \\ l_{ij,t} - v_{ij,t} \end{matrix} \right\|_2 \le l_{ij,t} + v_{i,t} \tag{16}$$

2) 5G BS and ESS Constraints

The electric power of the 5G BS backup batteries at each time interval is constrained by the electric power at the end of the previous time interval and the dispatchable capacity of the current time interval. The charging/discharging power of 5G BS is constrained by the output power of BS converter and power load at each time interval. Formula (17) is the upper limit constraint of charging/discharging power, which is affected by the electric load of 5G BS. Formula (18) is the capacity constraint of the backup batteries, which is limited by dispatchable capacity of 5G BS backup batteries. Formulas (17) and (18) are determined based on the evaluation results in Section II.

$$\begin{cases} b_{BS,j,a,t}^{dis} + b_{BS,j,a,t}^{ch} \le 1 \\ 0 \le P_{BS,j,a,t}^{ch} \le b_{BS,j,a,t}^{ch} P_{BS,j,a,t}^{ch,\max} \\ P_{BS,j,a,t}^{ch,\max} = P_{BS,j,a}^{conver} - P_{j,a,t}^{BS} \\ 0 \le P_{BS,j,a,t}^{dis} \le b_{BS,j,a,t}^{dis} P_{BS,j,a,t}^{dis,\max} \\ P_{BS,j,a,t}^{dis,\max} = P_{j,a,t}^{BS} \end{cases} \quad \forall j \in S^{BS} \tag{17}$$

$$\begin{cases} E_{j,t}^{BS,n} = \sum_{a=1}^{N_{j,t}^{BS,d}} SOC_{j,a,L,t}^{BS,n} \cdot E_{a,0}^{BS} \\ E_{j,t}^{BS} = E_{j,t_0}^{BS} + \sum_{a=1}^{N_{j,t}^{BS,d}} (\eta_{BS,j,a}^{ch} P_{BS,j,a,t}^{ch} - P_{BS,j,a,t}^{dis} / \eta_{BS,j,a}^{dis}) \\ E_{j,t_0}^{BS} = \max\{E_{j,t-1}^{BS}, E_{j,t}^{BS,n}\} \\ E_{j,t}^{BS,n} \le E_{j,t}^{BS} \le E_{j,t}^{BS,n} + E_{j,t}^{BS,d} \end{cases} \quad \forall j \in S^{BS} \tag{18}$$

ESS needs to consider the charging/discharging power constraints and the capacity timing relationship.

$$\begin{cases} b_{ESS,j,t}^{dis} + b_{ESS,j,t}^{ch} \le 1 \\ 0 \le P_{ESS,j,t}^{ch} \le b_{ESS,j,t}^{ch} P_{ESS,j}^{ch,\max} \\ 0 \le P_{ESS,j,t}^{dis} \le b_{ESS,j,t}^{dis} P_{ESS,j}^{dis,\max} \\ E_{j,t}^{ESS} = E_{j,t-1}^{ESS} + \eta_{ESS,j}^{ch} P_{ESS,j,t-1}^{ch} - P_{ESS,j,t-1}^{dis} / \eta_{ESS,j}^{dis} \\ E_j^{ESS,\min} \le E_{j,t}^{ESS} \le E_j^{ESS,\max} \end{cases} \quad \forall j \in S^{ESS} \tag{19}$$

3) Constraints of Other Voltage Regulation Resources

The operation constraints of PVs, SVCs, OLTCs, and CBs can be expressed as (20)-(23), respectively.

$$(P_{j,t}^{PV})^2 + (Q_{j,t}^{PV})^2 \le (S_j^{PV})^2 \quad \forall j \in S^{PV} \tag{20}$$

$$Q_j^{SVC,\min} \le Q_{j,t}^{SVC} \le Q_j^{SVC,\max} \quad \forall j \in S^{SVC} \tag{21}$$

$$\begin{cases} v_{j,t} = v_{pri,t} \left(k_{\min} + \sum_s k_s a_{s,j,t}^{OLTC} \right) \\ a_{s,j,t}^{OLTC} \le a_{s-1,j,t}^{OLTC} \quad s \in [2, N_{OLTC}^{\max}] \\ n_{j,t}^{OLTC} \le N_{OLTC}^{\max} \\ n_{j,t}^{OLTC} = \sum_s a_{s,j,t}^{OLTC} \\ n_{j,t}^{OLTC} - n_{j,t-1}^{OLTC} \le N_{OLTC}^{\max} b_{OLTC,j,t}^{IN} - b_{OLTC,j,t}^{DE} \\ n_{j,t}^{OLTC} - n_{j,t-1}^{OLTC} \ge b_{OLTC,j,t}^{IN} - N_{OLTC}^{\max} b_{OLTC,j,t}^{DE} \\ b_{OLTC,j,t}^{IN} + b_{OLTC,j,t}^{DE} \le 1 \\ \sum_{t \in T} (b_{OLTC,j,t}^{IN} + b_{OLTC,j,t}^{DE}) \le \Delta n_{j,T}^{OLTC,\max} \end{cases} \quad \forall j \in S^{OLTC} \tag{22}$$

$$\begin{cases} Q_{j,t}^{CB}=q_{step}^{CB}n_{j,t}^{CB} \\ a_{s,j,t}^{CB}\le a_{s-1,j,t}^{CB} \quad s\in[2,N_{CB}^{\max}] \\ n_{j,t}^{CB}=\sum_{s}a_{s,j,t}^{CB} \\ n_{j,t}^{CB}\le N_{CB}^{\max} \\ n_{j,t}^{CB}-n_{j,t-1}^{CB}\le N_{CB}^{\max}b_{CB,j,t}^{IN}-b_{CB,j,t}^{DE} \\ n_{j,t}^{CB}-n_{j,t-1}^{CB}\ge b_{CB,j,t}^{IN}-N_{CB}^{\max}b_{CB,j,t}^{DE} \\ b_{CB,j,t}^{IN}+b_{CB,j,t}^{DE}\le 1 \\ \sum_{t\in T}(b_{CB,j,t}^{IN}+b_{CB,j,t}^{DE})\le \Delta n_{j,T}^{CB,\max} \end{cases} \quad \forall j\in S^{CB} \tag{23}$$

The variable definitions of CB are similar to those of OLTC and will not be repeated here.

IV. Incentive Policy for 5G BS to Participate in ADN Voltage Optimization

A. Analysis of Benefit Condition for ADN

The dispatchable capacity of 5G BS backup batteries that can be used for voltage profile optimization is a new flexible resource in ADN, which makes it possible for 5G BS operators and ADN to achieve a win-win situation.

In this paper, two schemes are set up to analyze the economic advantages of 5G BS backup batteries participating in the voltage profile optimization of ADN at interval τ. The voltage regulation amplitude is the same for both schemes. The types and capacities of other flexible resources are identical, except for the composition of energy storage.

1) Scheme 1: only ESS participates in voltage profile optimization. The charging electric power and discharging electric power of node j ESS are $E_j^{ESS,ch}$ and $E_j^{ESS,dis}$, respectively.

2) Scheme 2: both ESS and 5G BS backup batteries participate in voltage profile optimization. The charging electric power and discharging electric power of ESS for node j are $(1-a)E_j^{ESS,ch}$ and $(1-b)E_j^{ESS,dis}$, respectively. The charging electric power and discharging electric power of backup batteries for node j are $aE_j^{ESS,ch}$ and $bE_j^{ESS,dis}$, respectively. This paper considers the electric power of backup batteries aggregated at node j, and does not consider the distribution electric power of electric power among 5G BSs.

The costs of the two schemes, i.e., F_{sce1} and F_{sce2}, are expressed as:

$$\begin{cases} F_{sce1}=C_{ESS}(E_j^{ESS,ch}+E_j^{ESS,dis}) \quad \forall j\in S^{CB} \\ F_{sce2}=C_{ESS}[(1-a)E_j^{ESS,ch}+(1-b)E_j^{ESS,dis}]+ \\ \qquad C_{ch,\tau}^{BS}aE_j^{ESS,ch}+C_{dis,\tau}^{BS}bE_j^{ESS,dis} \quad \forall j\in S^{BS}\bigcap S^{ESS} \end{cases} \tag{24}$$

The cost savings of scheme 2 compared with that of scheme 1 can be expressed as:

$$F_{j,ADN}=xaE_j^{ESS,ch}+ybE_j^{ESS,dis} \tag{25}$$

where $x=C_{ESS}-C_{ch,\tau}^{BS}$; and $y=C_{ESS}-C_{dis,\tau}^{BS}$.

If $F_{j,ADN}>0$, we can get:

$$\begin{cases} \dfrac{x}{y}>-\dfrac{bE_j^{ESS,dis}}{aE_j^{ESS,ch}} & y>0 \\ \dfrac{x}{y}<-\dfrac{bE_j^{ESS,dis}}{aE_j^{ESS,ch}} & y<0 \end{cases} \tag{26}$$

Formula (26) is the benefit condition of ADN. Suppose $E_j^{ESS,ch}$ and $E_j^{ESS,dis}$ are equal to 60 and 40 kWh, respectively. Figure 6 shows cost savings of ADN $F_{j,ADN}$ with different a and b values. As can be observed from Fig. 6, if $y>x$ and $y>0$, the more discharging capacity allocated by 5G BS backup batteries, the more cost of ADN can be saved; if $y<x$ and $x>0$, the more charging capacity allocated by 5G BS, the more cost of ADN can be saved. For the ADN, the larger the values of x and y, the more cost will be saved. However, the excessive values of x and y will damage the interests of 5G BS operators.

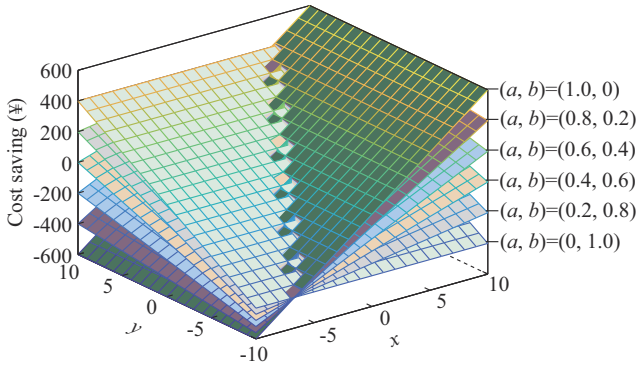

Fig. 6. Cost savings of ADN with different a and b values.

B. Analysis of Benefit Condition for 5G Operators

Under scheme 2, the revenue of 5G operators can be expressed as:

$$F_{j,ope}=C_{ch}^{BS}aE_j^{ESS,ch}+C_{dis}^{BS}bE_j^{ESS,dis}-F_{j,deg} \tag{27}$$

5G BS backup batteries frequently participate in the voltage profile optimization of ADN by charging and discharging, which inevitably aggravates the degradation of batteries. For the 5G operators, the revenue from ADN needs to be greater than the degradation cost of backup batteries, i.e.,

$$F_{j,deg}<(C_{ESS}-x)aE_j^{ESS,ch}+(C_{ESS}-y)bE_j^{ESS,dis} \tag{28}$$

The battery degradation characteristic is analyzed in [40]. The results show that the cycle life of batteries is directly related to the depth of charging/discharging (DoD), a parameter that can be used to determine the battery degradation cost. DoD can be expressed as:

$$DoD_{BS,j,a}^{(\cdot)}=\frac{P_{BS,j,a,t}^{(\cdot)}\Delta\tau}{E_{a,0}^{BS}} \tag{29}$$

where $DOD_{BS,j,a}^{(\cdot)}=DOD_{BS,j,a}^{ch}/DOD_{BS,j,a}^{dis}$; and $P_{BS,j,a,t}^{(\cdot)}=P_{BS,j,a,t}^{ch}/P_{BS,j,a,t}^{dis}$.

Equation (30) shows the relationship between the degradation cost coefficient and DoD [41].

$$C_{BS,j,a}^{deg}=\frac{F_{re,BS}}{2A(DoD_{BS,j,a}^{(\cdot)})^{-B}\mathrm{e}^{-C\cdot DoD_{BS,j,a}^{(\cdot)}}\eta_{BS,j,a}^{ch}\eta_{BS,j,a}^{dis}}=f(DoD_{BS,j,a}^{(\cdot)}) \tag{30}$$

where A, B, and C are the function coefficients.

Further, $F_{j,deg}$ can be expressed as:

$$\begin{cases} F_{j,deg} = \sum_{a=1}^{N_{j,t}^{BS,d}} C_{BS,j,a}^{deg}\left(E_{BS,j,a}^{ch} + E_{BS,j,a}^{dis}\right) \\ \sum_{a=1}^{N_{j,t}^{BS,d}} E_{BS,j,a}^{ch} = aE_j^{ESS,ch} \\ \sum_{a=1}^{N_{j,t}^{BS,d}} E_{BS,j,a}^{dis} = bE_j^{ESS,dis} \end{cases} \tag{31}$$

It is assumed that the degradation cost coefficient of each 5G BS for node j is equal. It is noteworthy that the charging/discharging behavior of 5G BS backup batteries is difficult to keep consistent in the actual operation, so the degradation cost coefficient of 5G BS is unequal. Under this assumption, substituting (31) into (28) yields:

$$\begin{cases} C_{BS,j,a}^{deg} < C_{ESS} - C_{j,ADN} \\ C_{j,ADN} = x + (y-x)\dfrac{bE_j^{ESS,dis}}{aE_j^{ESS,ch} + bE_j^{ESS,dis}} \end{cases} \tag{32}$$

where $C_{ESS} - C_{j,ADN}$ is the benefit coefficient obtained by the 5G BS from node j of ADN.

Formula (32) is the benefit condition of 5G operators. Suppose $E_j^{ESS,ch}$ and $E_j^{ESS,dis}$ are equal to 60 and 40 kWh, respectively. Let $C_{BS,j,a}^{deg} = C_{j,ADN}$. Figure 7 shows the degradation cost coefficient of 5G BS under different a and b values. As can be observed from Fig. 7, the area above the plane can guarantee that $C_{BS,j,a}^{deg} > C_{j,ADN}$, and the x and y values of this area can make 5G operators benefit from ADN.

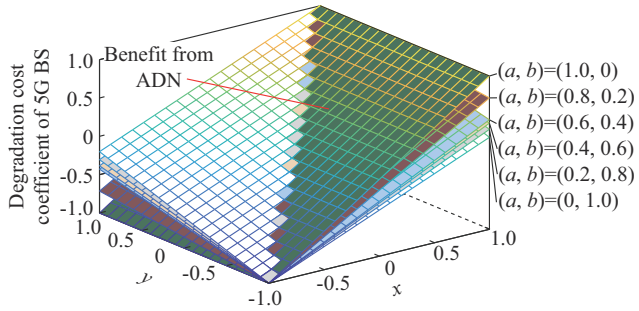

Fig. 7. Variation of degradation cost coefficient for 5G BS with different a and b values.

C. Incentive Policy for 5G Operators

Declaration The definitions of variables are the same as in the previous two subsections, with an additional time-varying property. For example, $C_{ESS,t}$ represents the cost coefficients of ESS at t.

This subsection presents a dynamic incentive policy to guide 5G operators to participate in the voltage profile optimization of ADN. On the premise of ensuring the absolute benefits of 5G operators, the charging/discharging tasks undertaken by the ESS are redistributed to 5G BSs, thereby reducing the ESS cost of ADN and realizing a win-win situation for ADN and 5G operators. The principles of this incentive policy are as follows.

Principle 1: in any interval, $x_t < 0$ and $y_t < 0$ are not satisfied simultaneously.

Principle 2: in any interval, $C_{ESS,t} - x_t < C_{BS,j,t}^{deg,\max}$ and $C_{ESS,t} - y_t < C_{BS,j,t}^{deg,\max}$ are not satisfied simultaneously.

Principle 3: in any interval, $C_{BS,j,t}^{deg,\max} < C_{ESS,t} - C_{ADN,j,t}$. $C_{BS,j,t}^{deg,\max}$ can be expressed as:

$$C_{BS,j,t}^{deg,\max} = \max\left\{f\left(DoD_{BS,j,t}^{(\cdot),up}\right)\right\} \tag{33}$$

Among them, Principle 1 ensures that ADN has a feasible benefit plan at any interval, which is derived from the benefit condition of ADN. Principle 2 ensures that 5G operators have a feasible benefit plan at any interval, which is derived from the degradation characteristic of backup batteries. Principle 3 is an absolute benefit condition for 5G operators, which can be further expressed as:

$$\begin{cases} \dfrac{\lambda_1(t)}{\lambda_1(t)+\lambda_2(t)}x_t + \dfrac{\lambda_2(t)}{\lambda_1(t)+\lambda_2(t)}y_t < h\left(C_{BS,j,t}^{deg,\max}\right) \\ \lambda_1(t) = a_t E_{j,t}^{ESS,ch} \\ \lambda_2(t) = b_t E_{j,t}^{ESS,dis} \\ h\left(C_{BS,j,t}^{deg,\max}\right) = C_{ESS,t} - C_{BS,j,t}^{deg,\max} \end{cases} \tag{34}$$

where $\lambda_1(t)$ and $\lambda_2(t)$ represent the charging and discharging electric power redistributed to 5G BS from the task undertaken by ESS, respectively, and they are fixed positive values at each interval. $h\left(C_{BS,j,t}^{deg,\max}\right)$ is a fixed value at each interval, and its value has three situations, i.e., ① situation 1: $h\left(C_{BS,j,t}^{deg,\max}\right) > 0$; ② situation 2: $h\left(C_{BS,j,t}^{deg,\max}\right) = 0$; ③ situation 3: $h\left(C_{BS,j,t}^{deg,\max}\right) < 0$.

Figure 8 shows the analysis of a win-win situation between 5G operators and ADN, where Lines 1, 2, and 3 correspond to the above three situations, respectively. As can be observed from Fig. 8, Zone 1 is the area satisfies (34) under situation 1. The area above Line 1 that satisfies (26) under situation 2. Zone 4 is the area that satisfies (34) under situation 3. Among them, the values of x_t and y_t in Zone 1 and Zone 4 can ensure the benefit of 5G operators, the values of x_t and y_t in this area above Line 1 can ensure the benefit of ADN.

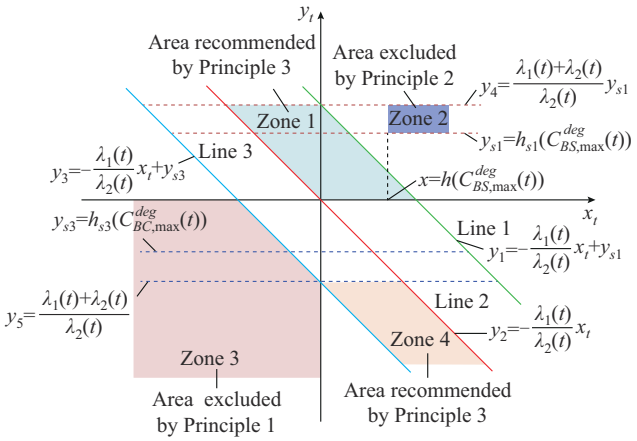

Fig. 8. Analysis of a win-win situation between 5G operators and ADN.

To achieve a win-win situation between 5G operators and ADN, the x_t and y_t values need to be determined in Zone 1. If (x_t, y_t) is located in the first quadrant of Zone 1, it is more beneficial to 5G operators, and charging can bring more benefits. If (x_t, y_t) is located in the second quadrant of Zone 1, it is more beneficial to ADN, and the closer to (0, 0), the greater cost savings of ADN. The area above Zone

1 is not a win-win zone for 5G operators and ADN. In particular, Zone 2 is excluded by Principle 2, and Zone 3 is excluded by Principle 1.

Lines 1, 2, and 3 are the three uncertain lines in Zone 1 envelope, which can be determined by $h(C_{BS,j,t}^{deg,\max})$, $\lambda_1(t)$, and $\lambda_2(t)$. The calculation method of these three parameters is given as follows.

1) Calculation of $h(C_{BS,j,t}^{deg,\max})$

Step 1: evaluate the dispatchable capacity of 5G BS backup batteries, and the evaluation method is given in Section II-D.

Step 2: calculate the upper limit of the 5G BS DoD value for node j at t according to (35).

$$\begin{cases} DoD_{BS,j,t}^{ch,up} = \min\left\{ \dfrac{P_{BS,j,a,t}^{ch,\max}\Delta\tau}{E_{a,0}^{BS}}, 1 - SOC_{j,a,L,t}^{BS,n} \right\} \\ DoD_{BS,j,t}^{dis,up} = \min\left\{ \dfrac{P_{BS,j,a,t}^{dis,\max}\Delta\tau}{E_{a,0}^{BS}}, 1 - SOC_{j,a,L,t}^{BS,n} \right\} \end{cases} \tag{35}$$

Step 3: calculate $C_{BS,j,t}^{deg,\max}$ according to (33).

Step 4: calculate $h(C_{BS,j,t}^{deg,\max})$ according to (34).

2) Calculation of $\lambda_1(t)$ and $\lambda_2(t)$

Step 1: determine $E_{j,t}^{ESS,ch}$ and $E_{j,t}^{ESS,dis}$ according to (34). This value is calculated in the scenario where only ESS undertakes the charging/discharging task.

$$\begin{cases} E_{j,t}^{ESS,ch} = E_{j}^{ESS,\max} - E_{j,t-1}^{ESS} \\ E_{j,t}^{ESS,dis} = E_{j,t-1}^{ESS} - E_{j}^{ESS,\min} \end{cases} \tag{36}$$

Step 2: calculate a_t and b_t according to (37).

$$\begin{cases} a_t = \dfrac{N_{j,t}^{BS,d} E_{a,0}^{BS} \cdot DoD_{BS,j,t}^{ch,up}}{E_{j,t}^{ESS,ch} + N_{j,t}^{BS,d} E_{a,0}^{BS} \cdot DoD_{BS,j,t}^{ch,up}} \\ b_t = \dfrac{N_{j,t}^{BS,d} E_{a,0}^{BS} \cdot DoD_{BS,j,t}^{dis,up}}{E_{j,t}^{ESS,dis} + N_{j,t}^{BS,d} E_{a,0}^{BS} \cdot DoD_{BS,j,t}^{dis,up}} \end{cases} \tag{37}$$

Step 3: calculate $\lambda_1(t)$ and $\lambda_2(t)$ according to (34).

After $h(C_{BS,j,t}^{deg,\max})$, $\lambda_1(t)$, and $\lambda_2(t)$ are determined, the incentive policy area that can achieve a win-win situation between 5G BS and ADN can be obtained. Under this incentive policy, the feasible areas of $C_{ch,t}^{BS}$ and $C_{dis,t}^{BS}$ vary with the dispatchable capacity of 5G BS backup batteries. Therefore, this is a dynamic incentive policy, which can achieve a win-win situation between ADN and 5G operators at each interval. However, this incentive policy is only used to determine a reasonable range of values for x_t and y_t.

D. Voltage Optimization Process of ADN with 5G BS

Figure 9 shows the process of 5G BS participating in voltage profile optimization, which requires coordination between the evaluation system, 5G operators, and ADN.

$E_{j,t}^{BS,n}$ and $E_{j,t}^{BS,d}$ are evaluated and transmitted to the 5G operators and ADN in the evaluation system. 5G operators determine whether to participate in the voltage profile optimization of ADN based on the current electric power and the maximum degradation cost coefficient of 5G BS. If participating, the $C_{BS,j,t}^{deg,\max}$, a_t, and b_t are calculated and sent to ADN, which are the three key parameters used to determine Zone 1. At the same time, the 5G BS constraints are introduced into the voltage profile optimization model for ADN.

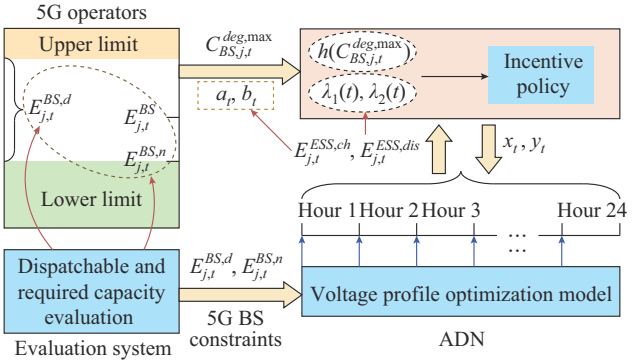

Fig. 9. Process of 5G BS participating in voltage profile optimization.

V. Case Studies

A. Test System and Parameter Settings

In this paper, an improved ADN is used, and the network parameters are shown in [42]. Flexibility resources (including 5G BS backup batteries, ESSs, PVs, SVCs, CBs, and OLTCs) in voltage profile optimization are added to the original network. As shown in Fig. 10, the basic network is divided into residential area, commercial area, and office area. The parameter settings of the network are shown Tables I and II. The model parameter settings are shown in Table III. The simulations are conducted in MATLAB 2018a on a 64-bit computer with a 3.0 GHz CPU and 16.0 GB RAM. The optimization models are programmed on the YALMIP platform, and the MISOCP is solved by the CPLEX solver.

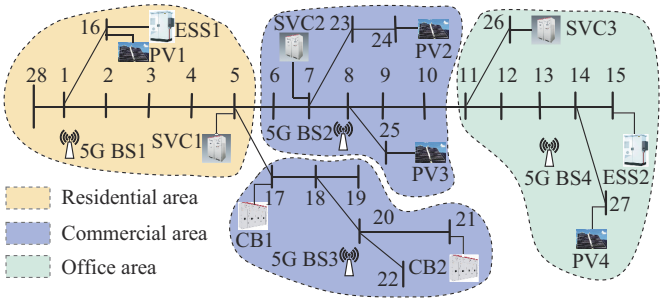

Fig. 10. A real distribution network topology.

TABLE I
Parameters of Voltage Regulation Devices

Resource	Per tap/capacity	Limit of times	Placement (bus No.)
OLTC	0.001 p.u.	5	28
CB	100 kvar	5	17, 21
SVC	300 kvar		5, 7, 26
PV	400 kVA		16, 23, 24, 27

B. Evaluation Results of Electric Load and Dispatchable Capacity for 5G BS Backup Batteries

In Fig. 11, each node is connected to 8-12 5G BSs, and each 5G BS is equipped with a set of 48 V/400 A·h backup batteries. When the reliability index of 5G BS and reliability rate of 5G BS backup batteries are 99.999% and 95%, respectively, the value of $T_{a,d}$ is 2.68 hours [24].

TABLE II
PARAMETERS OF ENERGY STORAGE RESOURCES

Resource	Charging efficiency	Discharging efficiency	SOC limit	Placement (bus No.)
ESS	0.9	0.9	[0.18, 0.9]	15, 16
5G BS1	0.9	0.9	To be evaluated	1-5, 16, 28
5G BS2	0.9	0.9		6-10, 23-25
5G BS3	0.9	0.9		17-22
5G BS4	0.9	0.9		11-15, 26-27

TABLE III
PARAMETERS OF OPTIMIZATION MODEL

Parameter	Value	Parameter	Value
C_{loss} (¥/kWh)	0.3	$[v_{j,\min}, v_{j,\max}]$	$[0.95^2, 1.05^2]$
C_{ESS} (¥/kWh)	0.72	$\Delta n_{j,T}^{OLTC,\max}$	5
C_Q^{SVC} (¥/kWh)	600	$N_{OLTC}^{\max}$	12
C_{CB} (¥/tap)	100	$\Delta n_{j,T}^{CB,\max}$	5
C_{OLTC} (¥/tap)	10	$N_{CB}^{\max}$	10
$P_{ESS,j}^{dis,\max}$ (kW)	300	$P_{ESS,j}^{ch,\max}$ (kW)	200

According to the method in Section II-D, the electric load of 5G BS, the dispatchable capacity of 5G BS backup batteries, and the maximum charging/discharging power of backup batteries are forecasted and evaluated.

1) In areas and time intervals with heavy electric loads, the dispatchable capacity of 5G BS backup batteries is small.

2) Due to the tidal effect of users, the dispatchable capacity of 5G BS backup batteries in office area increases greatly after work (hour 17), but decreases slightly in business area. At night (hours 23-6), the backup batteries in business area and office area have a large amount of dispatchable capacity, up to 78%.

3) The change of 5G service demand structure of users in office area leads to a larger fluctuation range (7.2%-67.6%) of dispatchable capacity of 5G BS backup batteries.

4) Compared to the day time, the maximum charging power of backup batteries is larger at night, while the maximum discharging power is smaller.

Substituting the maximum charging/discharging power and dispatchable capacity of 5G BS backup batteries into (22), (25), and (27) (where $A=4980$, $B=1.98$, $C=0.016$ [43]) to calculate the maximum degradation cost coefficient of 5G BS $C_{BS,j,t}^{deg,\max}$, the result is shown in Fig. 12. As can be observed from Fig. 12, $C_{BS,j,t}^{deg,\max}$ does not exceed 0.2 ¥/kWh, which makes $h(C_{BS,j,t}^{deg,\max})>0$ hold at any interval and node, which confirms that the existence of a win-win incentive policy zone for ADN and 5G operators. The minimum value of $C_{BS,j,t}^{deg,\max}$ is less than 0.05 ¥/kWh, which occurs at around hour 15. This is because the dispatchable capacity of 5G BS backup batteries at this interval is small. 5G BS will benefit from voltage profile optimization of ADN at around hour 15, which reflects the demand of ADN for voltage regulation resources (ADN voltage violation is more serious at around hour 15).

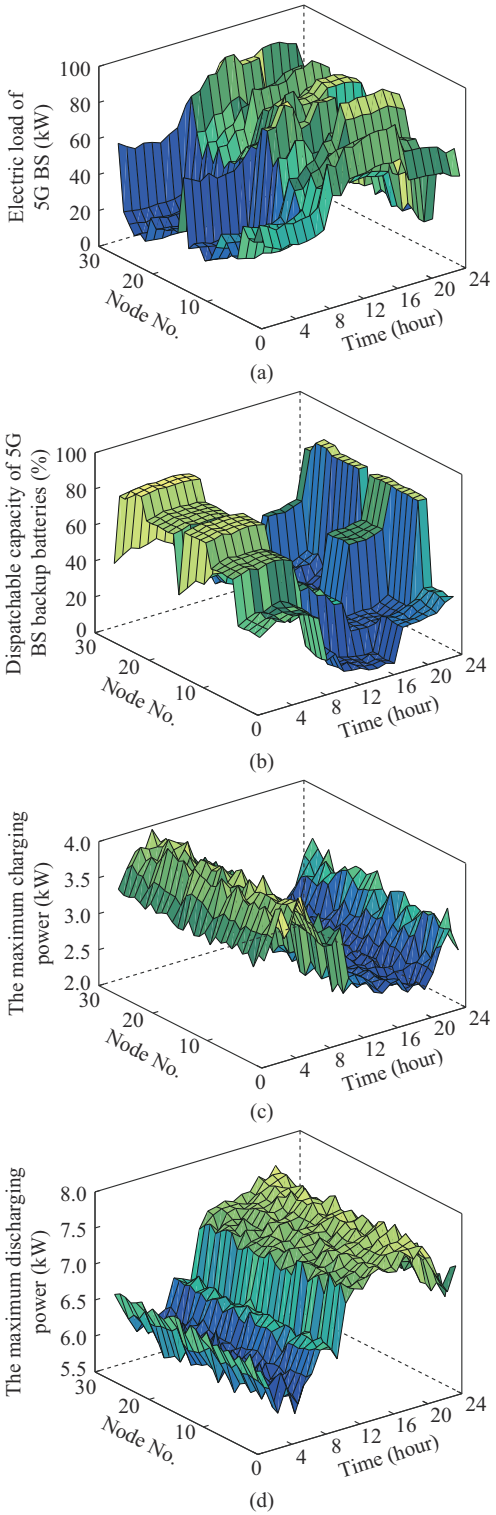

Fig. 11. Forecasted results of 5G BS. (a) Forecasted result of electric load. (b) Dispatchable capacity of 5G BS backup batteries. (c) The maximum charging power of a single 5G BS. (d) The maximum discharging power of a single 5G BS.

C. Optimization Effect of ADN Voltage Profile

Three scenarios are set to verify the effectiveness of dispatchable capacity of 5G BS backup batteries participating in the voltage profile optimization of ADN, as shown in Table IV.

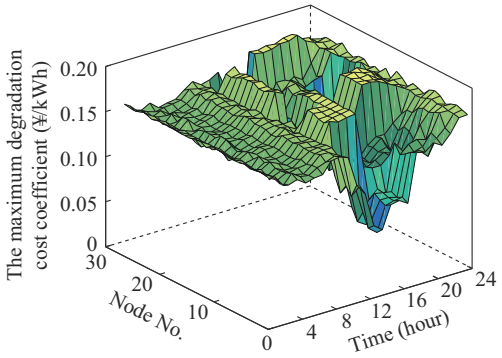

Fig. 12. The maximum degradation cost coefficient of 5G BS.

TABLE IV
RESOURCES PARTICIPATING IN VOLTAGE OPTIMIZATION IN THREE SCENARIOS

Scenario	OLTC	CB	SVC	PV	ESS	5G BG
1	√	√	√	√	×	×
2	√	√	√	√	√	×
3	√	√	√	√	√	√

Note: the symbols "√" and "×" represent that the resources are considered and not considered, respectively.

Figure 13 shows the comparison of voltage optimization results in three scenarios. In particular, scenario 3 only allows the 5G BSs of nodes 15 and 16 to participate in voltage profile optimization of ADN.

As can be observed from Fig. 13(a), affected by the inconsistent changes in PV output and electric load, the voltage exceeds the lower limit at night and exceeds the upper limit during the day time. The minimum voltage is only 0.926 p.u., while the maximum voltage reaches 1.132 p.u.. After the optimization, the ADN voltage profile has been significantly improved.

1) In Fig. 13(b), the voltage range is reduced to [1.032, 1.064]p.u., but the voltage of nodes still exceeds the upper limit during the daytime, especially the nodes close to OLTC (nodes 28, 1, and 16). This indicates that the allocation of resources in scenario 1 is difficult to consider both global and local voltage optimization, and more flexible resources need to be added to nodes with serious voltage violations to mitigate the impact of OLTC on global voltage.

2) In Fig. 13(c) and (d), the allocation of resources in scenarios 2 and 3 can make ADN voltage within a reasonable range, but the cost of scenario 3 is less. This indicates that 5G BS participates in the voltage profile optimization of ADN as an energy storage resource, reducing the cost of ESS in ADN.

Figures 14 and 15 show the cost analysis results of flexible resources in three scenarios. The cost coefficient of 5G BS used in scenario 3 will be explained in detail in the next subsection.

1) The costs of SVCs are the highest, accounting for 98%, 52%, and 71% in scenarios 1-3, respectively. It indicates that the large-capacity reactive power compensation or absorption is still the main method for voltage profile optimization of ADN.

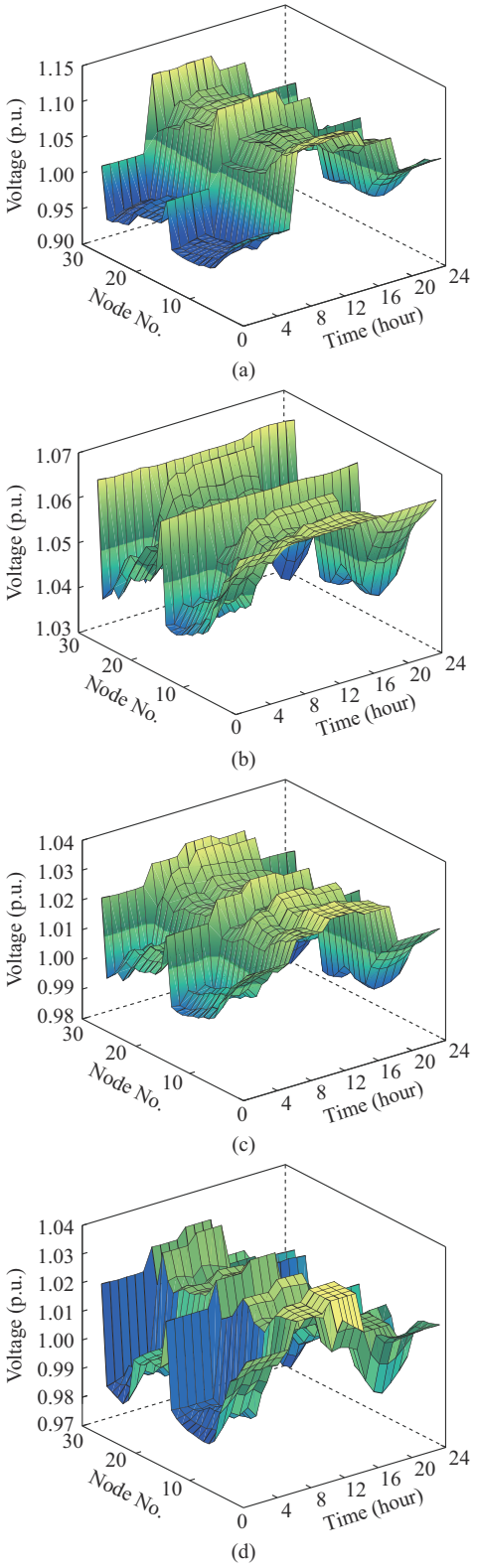

Fig. 13. Voltage optimization results of ADN. (a) Initial voltage profile. (b) Voltage profile in scenario 1. (c) Voltage profile in scenario 2. (d) Voltage profile in scenario 3.

2) The cost of the time interval including ESS is high, the cost of a single time interval is up to ¥991 (hour 19 in scenario 2), and the cost of ESS at a single time interval is up to ¥662 (hour 3 in scenario 2).

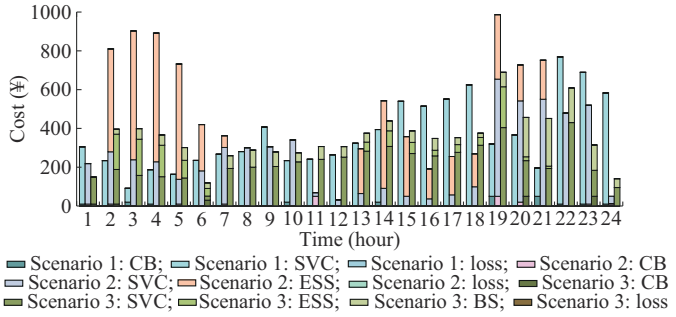

Fig. 14. Cost comparison of flexible resources in three scenarios.

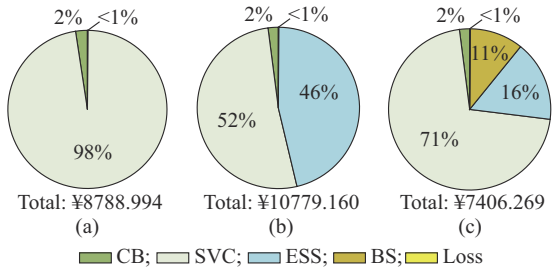

Fig. 15. Cost composition of flexible resources in three scenarios. (a) Scenario 1. (b) Scenario 2. (c) Scenario 3.

3) Comparing scenarios 2 and 1, the cost difference at a single time interval is mainly caused by ESS (hours 2-5 and 19), which indicates that ESS has a good effect on voltage optimization but is less economical.

4) The results in scenarios 2 and 3 show that, compared with other sources, the backup batteries are equally effective in voltage regulation and is more cost-efficient. After using the dispatchable capacity of 5G BS backup batteries, the same regulation effect is achieved, but the total cost is reduced from ¥10779.160 to ¥7406.269, and the costs of SVCs and ESS are reduced by 5.55% and 75.96%, respectively.

D. Analysis of Incentive Policy

The three key parameters that determine the win-win incentive policy area for ADN and 5G operators are shown in Fig. 16. According to the three parameters, the reasonable incentive policy areas of nodes 15 and 16 for each interval can be determined.

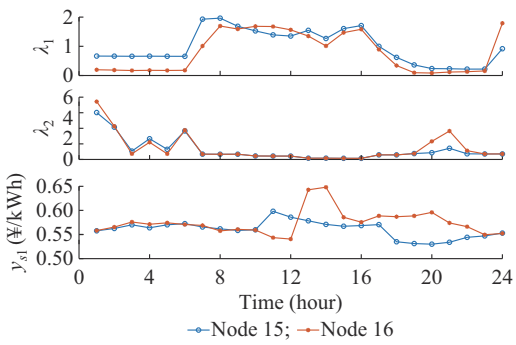

Fig. 16. Three key parameters to determine incentive policy area.

Further, as shown in Fig. 17, the cost coefficients of charging and discharging for 5G BS at nodes 15 and 16 are determined within a reasonable incentive policy area in combination with the difference in load characteristics. Figure 17 shows the incentive for ADN to guide 5G BS to participate in voltage profile optimization. ① At nodes 15 and 16, ADN expects 5G BS to participate in voltage profile optimization by charging during the period of hours 13-16, which is the peak PV output period. ② ADN expects the 5G BS located in the office area (node 16) to participate in voltage profile optimization by discharge during non-working periods.

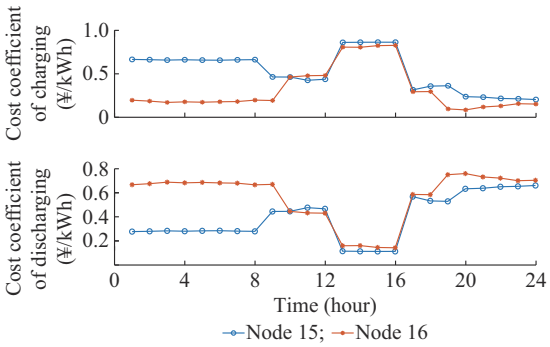

Fig. 17. Cost coefficients of charging and discharging for nodes 15 and 16.

In order to verify the effectiveness of the proposed incentive policy, this subsection allows the 5G BSs of all nodes to participate in the voltage profile optimization of ADN, and sets the following three incentive schemes.

Scheme 1: incentive policy proposed in this paper.

Scheme 2: constant incentive, where the cost coefficients of charging and discharging of all nodes are unchanged, and 5G BSs are regarded as conventional ESSs. The value is the average incentive value of scheme 1.

Scheme 3: multi-level incentives in different intervals [43]. The value is the average incentive value of each interval of scheme 1.

The cost coefficients of charging and discharging under schemes 2 and 3 are shown in Table V, and the cost coefficients of charging and discharging under scheme 1 is shown in Fig. 18.

TABLE V
COST COEFFICIENTS OF CHARGING AND DISCHARGING UNDER SCHEMES 2 AND 3

Scheme	State	Cost coefficient			
		23:00-06:00	06:00-12:00	12:00-17:00	17:00-22:00
2	Charging	0.407	0.407	0.494	0.407
	Discharging	0.494	0.494	0.407	0.494
3	Charging	0.654	0.436	0.632	0.265
	Discharging	0.561	0.454	0.307	0.613

The 5G BSs adjust ADN voltage to the distribution range of Fig. 13(c) and (d) in coordination with other voltage regulation resources. Under the three incentive schemes, the cost saving of ADN and the benefit of 5G operators are shown in Fig. 19.

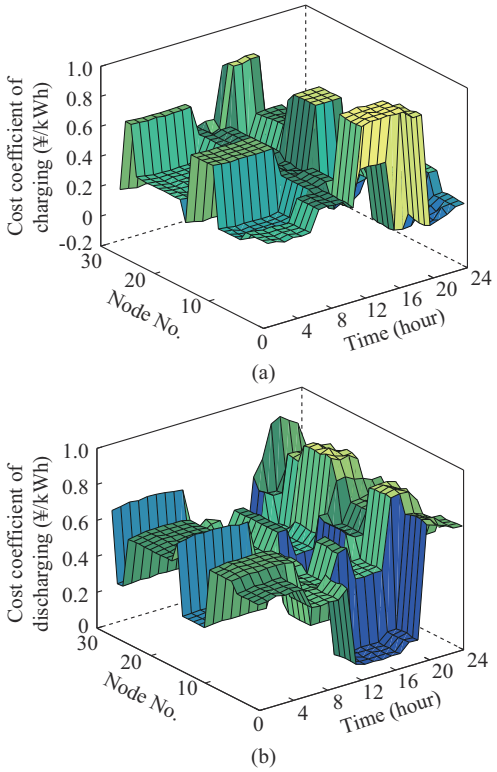

Fig. 18. Cost coefficients of charging and discharging under scheme 1.

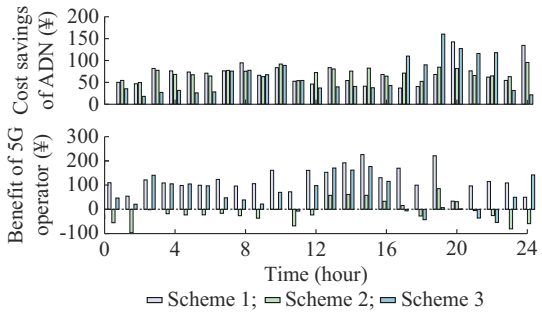

Fig. 19. Comparison of incentive policy effects under three incentive schemes.

As can be observed from Fig. 19, at some intervals, schemes 2 and 3 can save more costs for ADN but reduce the benefits of 5G operators. Only the incentive policy of scheme 3 can ensure that ADN and 5G operators can be in a win-win situation at any interval.

E. Influence of Dispatchable Capacity for 5G BS Backup Batteries

This subsection further analyzes the influence of dispatchable capacity for 5G BS backup batteries on the ADN voltage regulation effect. Taking Fig. 11(b) as a reference, in the case of only using 5G BS for voltage regulation, the voltage regulation effect at 120%, 100%, and 80% of the dispatchable capacity is analyzed, and the results are shown in Table VI.

It can be observed from Table V, a larger dispatchable capacity leads to a better voltage regulation effect, which indicates that 5G BS has the potential to participate in ADN voltage optimization on a large scale.

TABLE VI
COMPARISON OF VOLTAGE REGULATION EFFECTS OF DIFFERENT DISPATCHABLE CAPACITIES FOR 5G BS BACKUP BATTERIES

Dispatchable capacity (%)	Voltage range (p.u.)	Average voltage (p.u.)	Voltage standard deviation (p.u.)
80	[1.043, 1.114]	1.058	0.025
100	[1.035, 1.097]	1.046	0.022
120	[1.021, 1.083]	1.039	0.016

VI. CONCLUSION

To alleviate the voltage violation problem caused by PV in ADN, this paper proposes a voltage profile optimization method of ADN considering 5G BS backup batteries. The specific conclusions are as follows.

1) The evaluation method of electric load and dispatchable capacity of 5G BS backup batteries based on degrees of crowd aggregation is proposed for the first time. The evaluation results determine the charging/discharging behavior of 5G BS backup batteries in different areas at different time intervals. During the hours 20-24, commercial and office areas of 5G BSs are light-loaded, but the ADN is heavy-loaded, so the 5G BS backup batteries in those two areas can participate in voltage regulation by discharging. During the hours 0-8, 5G BSs and ADN are all light-loaded, 5G BS backup batteries can participate in voltage regulation by charging. During the day, the voltage regulation potential of commercial areas can be more fully exploited.

2) As an emerging flexible resource, the backup batteries of 5G BSs show great potential and advantages in providing voltage regulation services for ADN. Due to the significant aggregation and tidal effects, the backup batteries have larger capacity, stronger controllability and regularity, compared to other flexible resources (including PV, EV, air conditioner, etc.) in voltage regulation.

3) Under reasonable incentive policies, guiding 5G BS to participate in voltage optimization can not only improve the voltage management capability of ADN, and reduce the investment of ESS, but also bring additional benefits to 5G operators.

REFERENCES

[1] P. Li, C. Zhang, Z. Wu *et al*., "Distributed adaptive robust voltage/var control with network partition in active distribution networks," *IEEE Transactions on Smart Grid*, vol. 11, no. 3, pp. 2245-2256, May 2020.
[2] H. Sun, Q. Guo, J. Qi *et al*., "Review of challenges and research opportunities for voltage control in smart grids," *IEEE Transactions on Power Systems*, vol. 34, no. 4, pp. 2790-2801, Jul. 2019.
[3] A. Bharatee, P. K. Ray, and A. Ghosh, "A power management scheme for grid-connected PV integrated with hybrid energy storage system," *Journal of Modern Power Systems and Clean Energy*, vol. 10, no. 4, pp. 954-963, Jul. 2022.
[4] Y. Chai, L. Guo, C. Wang *et al*., "Hierarchical distributed voltage optimization method for HV and MV distribution networks," *IEEE Transactions on Smart Grid*, vol. 11, no. 2, pp. 968-980, Mar. 2020.
[5] X. Zhou, M. Farivar, Z. Liu *et al*., "Reverse and forward engineering of local voltage control in distribution networks," *IEEE Transactions on Automatic Control*, vol. 66, no. 3, pp. 1116-1128, Mar. 2021.
[6] J. Wang, N. Zhou, C. Y. Chung *et al*., "Coordinated planning of converter-based DG units and soft open points incorporating active management in unbalanced distribution networks," *IEEE Transactions on Sustainable Energy*, vol. 11, no. 3, pp. 2015-2027, Jul. 2020.

[7] W. Liao, J. Chen, Q. Liu *et al*., "Data-driven reactive power optimization for distribution networks using capsule networks," *Journal of Modern Power Systems and Clean Energy*, vol. 10, no. 5, pp. 1274-1287, Sept. 2022.
[8] H. Liu and W. Wu, "Two-stage deep reinforcement learning for inverter-based volt-var control in active distribution networks," *IEEE Transactions on Smart Grid*, vol. 12, no. 3, pp. 2037-2047, May 2021.
[9] H. Liu and W. Wu, "Online multi-agent reinforcement learning for decentralized inverter-based volt-var control," *IEEE Transactions on Smart Grid*, vol. 12, no. 4, pp. 2980-2990, Jul. 2021.
[10] S. Li, W. Hu, D. Cao *et al*., "Electric vehicle charging management based on deep reinforcement learning," *Journal of Modern Power Systems and Clean Energy*, vol. 10, no. 3, pp. 719-730, May 2022.
[11] T. M. Aljohani, A. Saad, and O. A. Mohammed, "Two-stage optimization strategy for solving the VVO problem considering high penetration of plug-in electric vehicles to unbalanced distribution networks," *IEEE Transactions on Industry Applications*, vol. 57, no. 4, pp. 3425-3440, Jul.-Aug. 2021.
[12] J. Liao, N. Zhou, Z. Qin *et al*., "Coordination control of power flow controller and hybrid DC circuit breaker in MVDC distribution networks," *Journal of Modern Power Systems and Clean Energy*, vol. 9, no. 6, pp. 1257-1268, Nov. 2021.
[13] H. Liang, J. Ma, and J. Lin, "Robust distribution system expansion planning incorporating thermostatically-controlled-load demand response resource," *IEEE Transactions on Smart Grid*, vol. 13, no. 1, pp. 302-313, Jan. 2022.
[14] H. S. V. S. K. Nunna, S. Battula, S. Doolla *et al*., "Energy management in smart distribution systems with vehicle-to-grid integrated microgrids," *IEEE Transactions on Smart Grid*, vol. 9, no. 5, pp. 4004-4016, Sept. 2018.
[15] Z. Chen, Y. Liu, X. Chen *et al*., "Charging and discharging dispatching strategy for electric vehicles considering characteristics of mobile energy storage," *Automation of Electric Power Systems*, vol. 44, no. 2, pp. 77-85, Jan. 2020.
[16] A. K. Barik and D. C. Das, "Coordinated regulation of voltage and load frequency in demand response supported biorenewable cogeneration based isolated hybrid microgrid with quasi-oppositional selfish herd optimization," *International Transactions on Electrical Energy Systems*, vol. 30, no. 1, pp. 1-22, Jan. 2020.
[17] P. Yong, N. Zhang, S. Ci *et al*., "5G communication base stations participating in demand response: key technologies and prospects," *Proceedings of the CSEE*, vol. 41, no. 16, pp. 5540-5551, Aug. 2021.
[18] S. Li, L. D. Xu, and S. Zhao, "5G Internet of Things: a survey," *Journal of Industrial Information Integration*, vol. 10, pp. 1-9, Jun. 2018.
[19] H. Hui, Y. Ding, Q. Shi *et al*., "5G network based Internet of Things for demand response in smart grid: a survey on application potential," *Applied Energy*, vol. 257, p. 113972, Jan. 2020.
[20] X. Liu, D. Zhang, Y. Xia *et al*., "A bandwidth enhancing 5G slotted antenna operating 3.5GHz with slitting patches," in *Proceedings of 2021 IEEE 4th International Conference on Electronic Information and Communication Technology (ICEICT)*, Xi'an, China, Aug. 2021, pp. 945-947.
[21] Northeast China Energy Regulatory Bureau of National Energy Administration. (2022, Mar.). Minister's Passage. [Online]. Available: https://news. cctv. com/2022/03/09/ARTItpY6rzDSGMV9kdNkOOoM220309.shtml
[22] China Center for Information Industry Development. (2020, Dec.). CCTV news. [Online]. Available: http://www. mtx. cn/#/report? id=684243
[23] C. Lin, S. Han, and S. Bian, "Energy-efficient 5G for a greener future," *Nature Electronics*, vol. 3, pp. 182-184, Apr. 2020.
[24] J. Wu, Y. Zhang, M. Zukerman *et al*., "Energy-efficient base-stations sleep-mode techniques in green cellular networks: a survey," *IEEE Communications Surveys & Tutorials*, vol. 17, no. 2, pp. 803-826, Jan. 2015.
[25] Z. Chang, Q. Gu, C. Lu *et al*., "5G private network deployment optimization based on RWSSA in open-pit mine," *IEEE Transactions on Industrial Informatics*, vol. 18, no. 8, pp. 5466-5476, Aug. 2022.
[26] X. Liu and Z. Bie, "Cooperative planning of distributed renewable energy assisted 5G base station with battery swapping system," *IEEE Access*, vol. 9, pp. 119353-119366, Sept. 2021.
[27] A. Dataesatu, P. Boonsrimuang, K. Mori *et al*., "Energy efficiency enhancement in 5G heterogeneous cellular networks using system throughput based sleep control scheme," in *Proceedings of 2020 22nd International Conference on Advanced Communication Technology (ICACT)*, Phoenix Park, Korea, Feb. 2020, pp. 549-553.
[28] Q. Wu, G. Y. Li, W. Chen *et al*., "An overview of sustainable green 5G networks," *IEEE Wireless Communications*, vol. 24, no. 4, pp. 72-80, Aug. 2017.
[29] 5G White Paper. (2015, Feb.). Next Gener. Mobile Netw. [Online]. Available: https://ngmn. org/wpcontent/uploads/NGMN_5G_White_Paper_V1_0.pdf
[30] S. Hu, X. Chen, W. Ni *et al*., "Modeling and analysis of energy harvesting and smart grid-powered wireless communication networks: a contemporary survey," *IEEE Transactions on Green Communications and Networking*, vol. 4, no. 2, pp. 461-496, Jun. 2020.
[31] C. Zhou, C. Feng, and Y. Wang, "Spatial-temporal energy management of base stations in cellular networks," *IEEE Internet of Things Journal*, vol. 9, no. 13, pp. 10588-10599, Jul. 2022.
[32] Y. Zou, Q. Wang, Y. Chi *et al*., "Electric load profile of 5G base station in distribution systems based on data flow analysis," *IEEE Transactions on Smart Grid*, vol. 13, no. 3, pp. 2452-2466, May 2022.
[33] P. Yong, N. Zhang, Q. Hou *et al*., "Evaluating the dispatchable capacity of base station backup batteries in distribution networks," *IEEE Transactions on Smart Grid*, vol. 12, no. 5, pp. 3966-3979, Sept. 2021.
[34] P. Yong, N. Zhang, Y. Liu *et al*., "Exploring the cellular base station dispatch potential towards power system frequency regulation," *IEEE Transactions on Power Systems*, vol. 37, no. 1, pp. 820-823, Jan. 2022.
[35] J. Li, Y. Feng, and Y. Hu, "Load forecasting of 5G base station in urban distribution network," in *Proceedings of 2021 IEEE 5th Conference on Energy Internet and Energy System Integration (EI2)*, Taiyuan, China, Oct. 2021, pp. 1308-1313.
[36] C. Fan, Z. Diao, and W. Liu, "Research on 5G power consumption and communication power supply scheme," *Communication World*, vol. 26, pp. 28-30, Sept. 2019.
[37] M. E. Leinonen, M. Jokinen, N. Tervo *et al*., "System EVM characterization and coverage area estimation of 5G directive W links," *IEEE Transactions on Microwave Theory and Techniques*, vol. 67, no. 12, pp. 5282-5295, Dec. 2019.
[38] M. E. Baran and F. F. Wu, "Optimal capacitor placement on radial distribution systems," *IEEE Transactions on Power Delivery*, vol. 4, no. 1, pp. 725-734, Jan. 1989.
[39] M. Farivar and S. H. Low, "Branch flow model: relaxations and convexification – Part I," *IEEE Transactions on Power Systems*, vol. 28, no. 3, pp. 2554-2564, Aug. 2013
[40] P. Wang, L. Goel, and Y. Xu, "A two-layer energy management system for microgrids with hybrid energy storage considering degradation costs," *IEEE Transactions on Smart Grid*, vol. 9, no. 6, pp. 6047-6057, Nov. 2018.
[41] S. Han, S. Han, and H. Aki, "A practical battery wear model for electric vehicle charging applications," *Applied Energy*, vol. 113, pp. 1100-1108, Jan. 2014.
[42] S. Li, H. Wu, Y. Zhou *et al*. (2022, Jan.). Two-stage voltage control strategy in distribution networks with coordinated multimode operation of PV inverters. [Online]. Available: https://doi.org/10.1049/rpg2.12421
[43] B. Wang, C. Zhang, and Z. Y. Dong, "Interval optimization based coordination of demand response and battery energy storage system considering SOC management in a microgrid," *IEEE Transactions on Sustainable Energy*, vol. 11, no. 4, pp. 2922-2931, Oct. 2020.

Yiyao Zhou received the B.S. degree from Chongqing University, Chongqing, China, in 2018, and the M.E. degree from Hefei University of Technology, Hefei, China, in 2021. He is currently pursuing his Ph. D. degree in School of Electrical Engineering, Chongqing University. His research interests include modeling, optimization and operation of distribution network.

Qianggang Wang received the B. S. and Ph. D. degrees from Chongqing University, Chongqing, China, in 2009 and 2015, respectively. He is currently an Associate Professor with the School of Electrical Engineering in Chongqing University. He was a Research Fellow with Nanyang Technological University, Singapore, from 2015 to 2016. His research interests include the analysis and operation of power systems, microgrids, and power quality.

Yao Zou received the B.E. and M.S. degrees from the College of Electrical and Information Engineering, Hunan University, Changsha, China, in 2015 and 2018, respectively. He is currently pursuing the Ph. D. degree with Chongqing University, Chongqing, China. From 2018 to 2020, he worked with State Grid Hunan Province Electric Power Company Maintenance Company. His current research interests include planning and operation of power system and integrated energy system.

Yuan Chi received the B.S. degree from Southeast University, Nanjing, Chi-

na, in 2009, the M.E. degree from Chongqing University, Chongqing, China, in 2012, and the Ph.D. degree from Nanyang Technological University, Singapore, in 2021. From 2012 to 2016, he worked as an Electrical Engineer of Power System Planning Consecutively with State Grid Chongqing Electric Power Research Institute and Chongqing Economic and Technological Research Institute, Chongqing, China. He is currently working as a Research Associate with Chongqing University. His research interests include planning and resilience of power system, and voltage stability.

Niancheng Zhou received the B.S., M.S., and Ph.D. degrees in electrical engineering from Chongqing University, Chongqing, China, in 1991, 1994, and 1997, respectively. He worked at Chongqing Kuayue Technology Co., Ltd., from 1997 to 2003. He is a Professor in School of Electrical Engineering, Chongqing University. From 2010 to 2011, he was a research fellow of Nanyang Technological University, Singapore. His research interests include analysis, operation of power system, microgrid, and power quality.

Xuefei Zhang received the B.S. and M.S. degrees in electrical engineering from Kunming University of Science and Technology, Kunming, China, in 2018 and 2021, respectively. He is currently pursuing the Ph.D. degree in School of Electrical Engineering, Chongqing University, Chongqing, China. His research interests include modeling, optimization, and operation of power system.

Chen Li received the B.S. degree from North China University of Water Resources and Electric Power, Zhengzhou, China, in 2015, and the M.S. degrees in electrical engineering from Chongqing University, Chongqing, China, in 2018, where he is currently working toward the Ph.D. degree. His research interests include renewable energy, power system operation, and power system planning.

Qinqin Xia received the B.E. degree from Southwest Petroleum University, Chengdu, China, in 2015, and the M.E. degree from Hunan University, Changsha, China, in 2019. She is currently pursuing the Ph.D. degree with Chongqing University, Chongqing, China. From 2019 to 2022, she worked with State Grid Chongqing Shibei Electric Power Supply Branch, Chongqing, China. Her current research interests include planning and operation of power system.